

Article

# Metamaterial-Based Highly Isolated MIMO Antenna for Portable Wireless Applications

Amjad Iqbal <sup>1,\*</sup> , Omar A Saraereh <sup>2</sup>, Amal Bouazizi <sup>3</sup> and Abdul Basir <sup>4</sup>

<sup>1</sup> Department of Electrical Engineering, CECOS University of IT and Emerging Sciences, Peshawar 25000, Pakistan

<sup>2</sup> Department of Electrical Engineering, The Hashemite University, Zarqa 13115, Jordan; eloas2@hu.edu.jo

<sup>3</sup> National Engineering School of Sfax, Electrical Engineering Department, Sfax 3038, Tunisia; amalbouazizi90@yahoo.fr

<sup>4</sup> Department of Biomedical Engineering, Hanyang University, Seoul 04763, Korea; engrobasir@hanyang.ac.kr

\* Correspondence: amjad730@gmail.com; Tel.: +92-344-8045575

Received: 6 September 2018; Accepted: 19 October 2018; Published: 22 October 2018



**Abstract:** In this paper, a metamaterial structure is presented to lower the mutual coupling between the closely spaced microstrip patch antenna elements. Two elements Multiple Input Multiple Output (MIMO) antenna is closely placed with each other at edge to edge separation of  $0.135\lambda_0$  (7 mm). Isolation improvement of 9 dB is achieved by keeping the metamaterial structure in between the MIMO elements. With the proposed structure, the isolation is achieved around  $-24.5$  dB. Due to low ECC, high gain, low channel capacity loss and very low mutual coupling between elements, the proposed antenna is a good candidate for the MIMO applications. The proposed antenna is fabricated and tested. A reasonable agreement between simulated and measured results is observed.

**Keywords:** MIMO; patch antenna; S-parameters; mutual coupling

## 1. Introduction

Currently, MIMO antenna has pulled a lot of attention due to its potential to enhance the capacity and reliability of the wireless communication system. In spite of its benefits, mutual coupling is a big challenge that needs to be overcome. Mutual coupling is typically undesirable since it affects the performance of the MIMO antenna and antenna array system. The interaction between the array elements/MIMO elements degrades the system performance by increasing mutual coupling, increasing envelop correlation coefficient, increasing channel capacity loss, decreasing diversity gain and distorting radiation pattern [1]. This problem may arise when antennas are placed nearby. MIMO antenna contains at least two spaced radiating elements in the aim of achieving good isolation between them. However, the available space is unsuitable for practical portable devices. In this respect, many techniques have been adopted to lower the mutual coupling between MIMO elements. In [2], by introducing F-shaped stubs in between the two radiators, the mutual coupling between the MIMO elements was decreased. Very reduced mutual coupling between the MIMO antennas is accomplished by utilizing neutralization line in [3]. Other approaches have been proposed in the literature to augment isolation between the radiators. Among the adopted approaches we can state the introduction of a meandered line resonator in between the radiating elements of the MIMO antenna [4], the use of different elements for polarization diversity [5], the use of electromagnetic bandgap structures [6–8], U-shaped radiator [9], defective ground structure [10]. Coupling between eye shaped MIMO antenna is reduced by utilizing extended T-shaped stub in between the two resonators [11]. In [12], Artificial Magnetic Conductor (AMC) is used below the V-shaped patches to achieve high gain, lower size and greater isolation. In [13], a novel shaped decoupling structure is inserted between the inverted F shaped radiating elements to lower the coupling.

It is in this context that the presented paper can be set with the aim of providing the design, prototyping, and measurement of a small size MIMO antenna. The latter contains two patches fed by a 3 mm wider microstrip lines. In the proposed design, the isolation is achieved by employing a series of metamaterial unit cells between the two antennas. The proposed antenna has a very low mutual coupling ( $|S_{21}/S_{12}| < -20$  dB). A comparison between simulated and measured results was inspected in the presented paper for the prototype validation. The proposed MIMO antenna is well-suited for the many wireless applications due to its low ECC, high diversity gain, high peak gain, low channel capacity loss and most of all, the very high isolation.

### 2. Antenna Characterization

The antenna model geometry is shown in Figure 1. The proposed antenna is printed on a low cost FR-4 substrate having a loss tangent and relative permittivity of 0.02 and 4.4, respectively. The proposed design has two patches excited using a 3 mm wider microstrip lines with a 50 Ω characteristic impedance. Edge to edge separation between the radiating elements of the MIMO antenna is kept as  $0.135\lambda_0$  (7 mm).

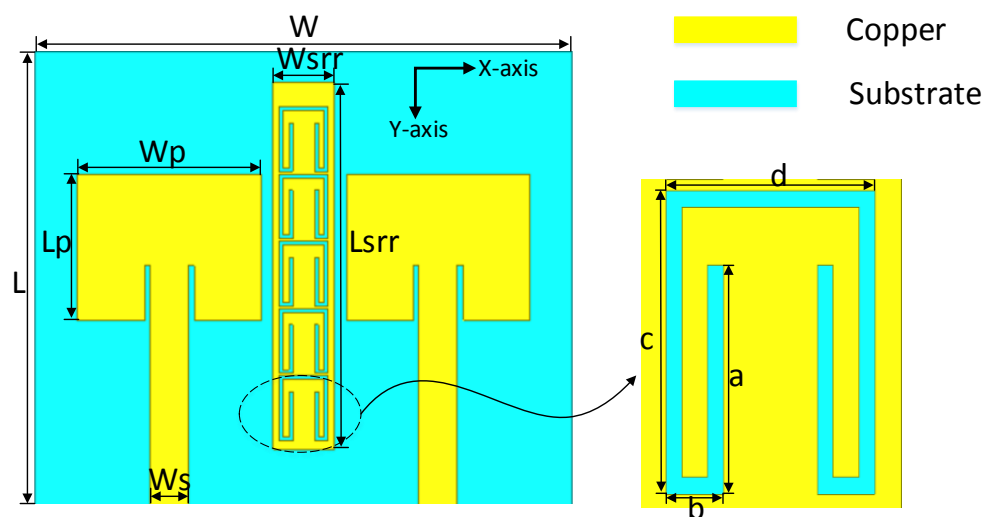


Figure 1. Top view of the proposed Multiple Input Multiple Output (MIMO) Antenna.

The proposed antenna’s associated parameters are provided in Table 1.

Table 1. Different Parameters and values of the antenna.

Parameters	Dimension (mm)	Parameters	Dimension (mm)	Parameters	Dimension (mm)
L	37	W	44	Ws	3
a	4	b	1.1	Lssr	30
Wp	15	c	5.3	d	4
Lp	13	Wssr	5	-	-

The iterative design process of the proposed MIMO antenna that includes three steps is presented in Figure 2.

Firstly, a single radiating element patch antenna with microstrip feed is designed and optimized to operate efficiently. Width and length of the optimized antenna were chosen as 15 mm and 13 mm respectively. Secondly, another patch antenna is designed near to the first one as shown in Figure 2 (step 2). The unit cell of the proposed metamaterial structure is shown in Figure 3b is used as decoupling structure. The unit cells are used between the antennas for a good isolation between the two antenna elements (step 3).

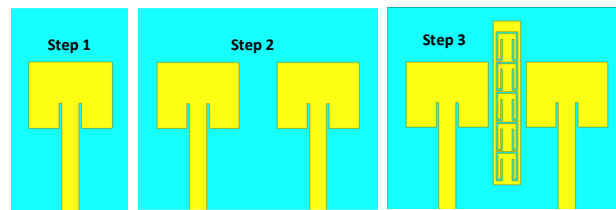


Figure 2. Steps for the design of proposed MIMO antenna.

Figure 3a presents the simulated reflection coefficient ( $S_{11}$ ) and the transmission coefficient ( $S_{21}$ ) of the proposed MIMO antenna with and without using metamaterial. It is clear from the Figure 3a that  $S_{11}$  of the MIMO antenna with and without metamaterial is almost same. The resonant frequency of MIMO antenna without metamaterial is observed at 5.7 GHz while the resonant frequency of the proposed MIMO antenna using metamaterial is observed at 5.8 GHz. It is worth highlighting that very low mutual coupling is constantly preferable for efficient MIMO antennas. Figure 3a shows that antenna without having metamaterial has poor isolation in the whole operating band. A very high isolation is achieved by employing metamaterial between the radiating elements.

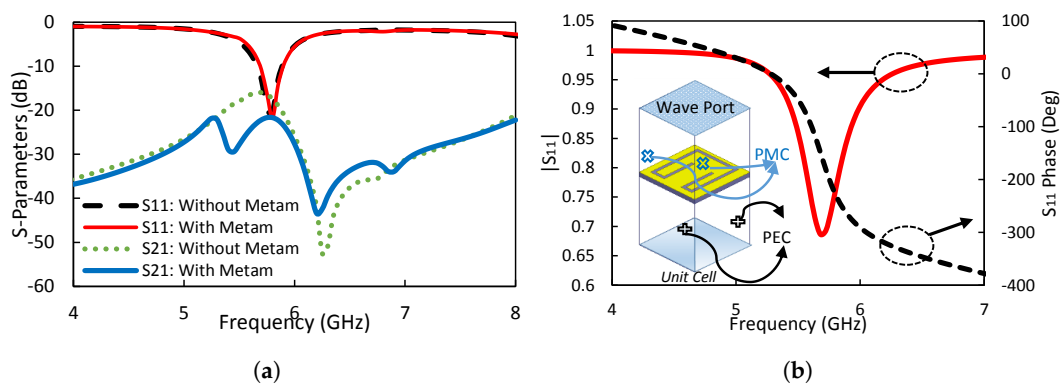


Figure 3. (a) Simulated S-parameter with and without metamaterial, (b) Unit Cell.

The isolation behavior can also be explained through the analysis of the antenna’s surface current distribution at the frequency of interest. The current distribution at 5.8 GHz in both cases (with and without using metamaterial) is presented in Figure 4. Upon excitation of port 1 of two port antenna, a high mutual coupling is obtained between the monopoles, because the current is strongly coupled to another radiator. It is obvious from the Figure 4 that mutual coupling is diminished by the insertion of metamaterial unit cells between the two radiating elements. Thus, a very low mutual coupling is achieved.

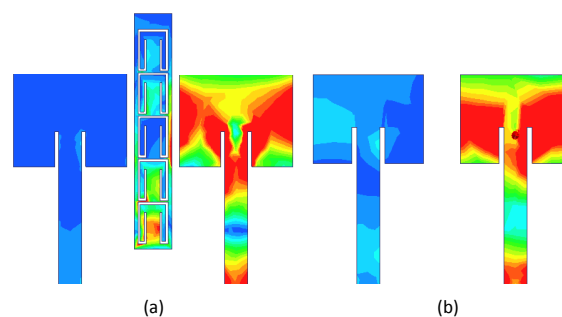


Figure 4. (a) Surface current distribution of MIMO antenna with metamaterial, (b) Surface current distribution without metamaterial.

To give a profound comprehension of the global configuration, the equivalent circuit model is provided in Figure 5. Three resonating structures are cascaded together. The patches of the proposed

antenna are modeled by a resonator structure with  $Lp1$ ,  $Cp1$ ,  $Lp2$ , and  $Cp2$ . The decoupling structure of metamaterial is modeled as  $LcR$ ,  $CcR$ , and  $RcR$ .  $Cc$  and  $Lc$  are coupling structures and help in the coupling of the two patches, which is always undesirable in MIMO antenna. The  $S_{21}$  of the proposed antenna is compared with the circuit model in Figure 6.

Table 2 presents the optimized parameters of the proposed circuit model.

The performances of the MIMO antenna are displayed in Table 3 comparing them to other antennas used in the literature.

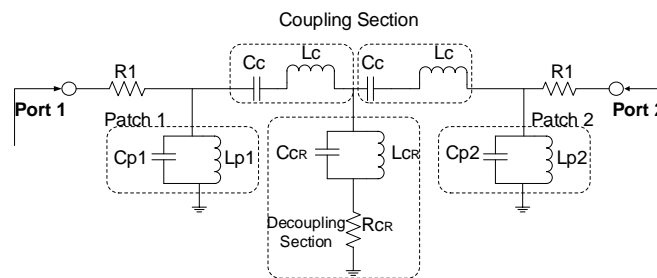


Figure 5. Equivalent Circuit Model of the proposed MIMO antenna.

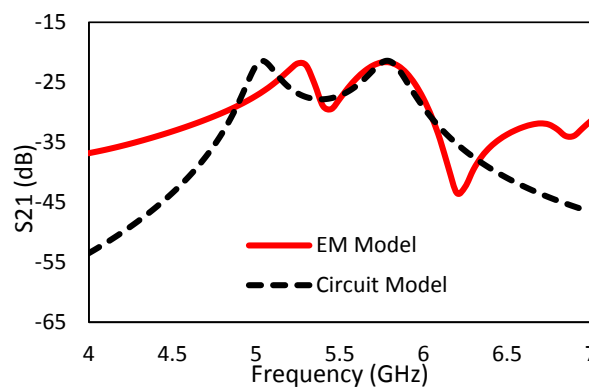


Figure 6.  $S_{21}$  comparison of EM model and circuit model of the proposed MIMO antenna.

Table 2. Optimized parameters of the circuit model.

R1 ( $\Omega$ )	Cc (pF)	Lc (nH)	Lp1/Lp2 (nH)	Cp1/Cp2 (pF)	CcR (pF)	LcR (nH)	RcR ( $\Omega$ )
466.75	1.2	2.15	0.83	1.31	0.01	0.64	0.01

Table 3. Performance comparison with previously published work.

Ref.	Technique	Isolation Improvement (dB)	Edge-Edge Distance	ECC	CCL (bits/s/Hz)
[7]	Dumbbell EBG	Not Given	Not Given	Not Given	Not Given
[8]	EBG	17	$0.47\lambda_0$	Not Given	Not Given
[9]	U-Shaped Resonator	6–10	$0.28\lambda_0$	Not Given	Not Given
Proposed Work	Metamaterial	9	$0.135\lambda_0$	<0.1	<0.05

### 3. Results and Discussions

To validate the proposed design, an antenna prototype is fabricated and measured. The antenna’s simulations were conducted using ANSYS High-Frequency Structure Simulator (HFSS) software. Figure 7 shows the antenna as fabricated in conformity with the aforementioned parameters. The antenna’s S-parameters were measured using an Agilent Network Analyzer (VNA). The measured S-parameters values are shown in Figure 7 for a comparison with the simulated results. Comparing the simulated and the measured results, we can notice that there is a slight frequency shift. This may be due to several factors which include the SMA connector loss, cable loss, limitation of milling machine as well as radiating boundaries during the measurement process. The measured frequency band

of the proposed MIMO antenna is within the range of 5.61–5.93 GHz with  $S_{11}/S_{22} < -10$  dB and  $S_{21}/S_{12} < -20$  dB.

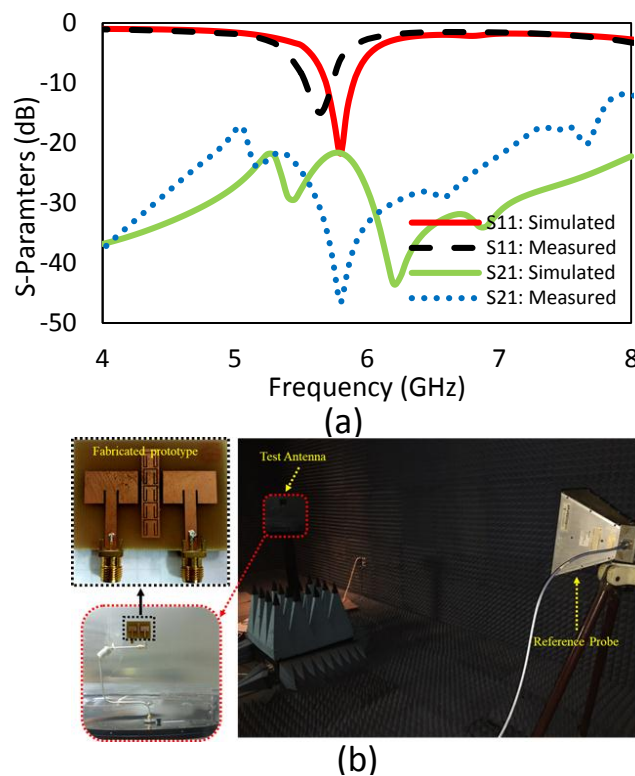


**Figure 7.** (a) Measured and simulated S-Parameters of the designed MIMO antenna, (b) Radiation pattern setup and fabricated antenna.

Further study mainly, in terms of the MIMO antenna’s radiation characteristics in both cases (with and without metamaterial) have also been conducted. Figure 8 display the simulated radiation patterns for both principal planes azimuthal ( $\Phi = 0$ ) and elevation ( $\Phi = 90$ ) at 5.8 GHz. As appeared in the figure, the introduction of metamaterial has a slight effect on the deviation of the radiation pattern.

The simulated peak gain of the proposed MIMO antenna with and without metamaterial as well as the measured peak gain is portrayed in Figure 9a. As shown in the figure, the antenna gain is enhanced when metamaterial unit cells are used and hence, the maximum realized peak gain of 4 dB is obtained at 5.8 GHz.

Isolation and correlation of communication channels can be observed from envelop correlation coefficient (ECC) value. ECC can be derived from the radiation pattern of all the antennas in a multi antenna system that how much radiation pattern of each antenna affect the radiation pattern of other antenna. Having a low ECC is very important to approve the robustness of the proposed MIMO antenna. For a uniform propagation scenario, The ECC can be computed using the following Formula [14].

$$ECC = \frac{|\iint_{4\pi} (\vec{F}_i(\theta, \phi)) \times (\vec{F}_j(\theta, \phi)) d\Omega|^2}{\iint_{4\pi} |(\vec{F}_i(\theta, \phi))|^2 d\Omega \iint_{4\pi} |(\vec{F}_j(\theta, \phi))|^2 d\Omega} \tag{1}$$

where  $\vec{F}_i(\theta, \Phi)$  describe the 3D radiation pattern when antenna  $i$  is excited and  $\vec{F}_j(\theta, \Phi)$  describe the 3D radiation pattern when antenna  $j$  is excited. Solid angle in above Equation (1) is represented as  $\Omega$ .

The ECC ought to have zero value in the ideal case. However, practical limit for an uncorrelated MIMO antenna is  $ECC < 0.5$ .

Figure 9b plots the simulated ECC between the two antennas resonating at 5.8 GHz. The ECC is around the ideal value and it is equal to 0.007 at 5.8 GHz. Furthermore, it is clear from the same figure that the ECC is less than 0.1 over the operating frequency band.

The Diversity Gain (DG) is another fundamental parameter, which characterizes the MIMO antenna. The DG can be calculated using the following equation [14].

$$DG = 10\sqrt{1 - (ECC)^2} \tag{2}$$

Figure 9b shows the DG versus frequency. At 5.8 GHz, the proposed MIMO antenna attained a DG of 9.3 dB. Yet, the proposed antenna has a DG > 9 dB over the entire operating band.

Another critical parameter for realizing the performance of MIMO antenna is its channel capacity loss (CCL). The CCL for any MIMO antenna can be computed using the following formula [15], where  $i, j = 1, 2$ .

The CCL calculated from S-Parameters is shown in Figure 10. As indicated in the figure, the proposed antenna achieves CCL values less than 0.5 bits/s/Hz.

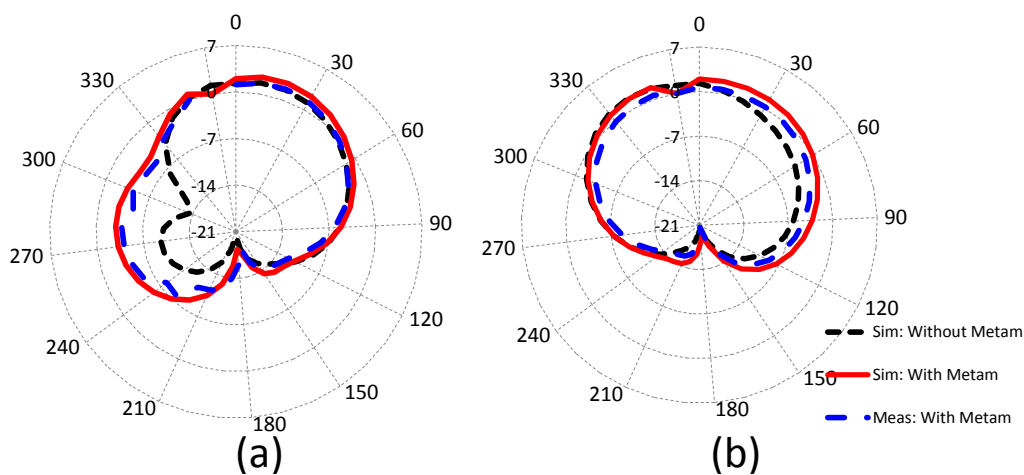


Figure 8. Measured and simulated radiation pattern(with and without metamaterial) at 5.8 GHz (a)  $\Phi = 0^\circ$ ; (b)  $\Phi = 90^\circ$ .

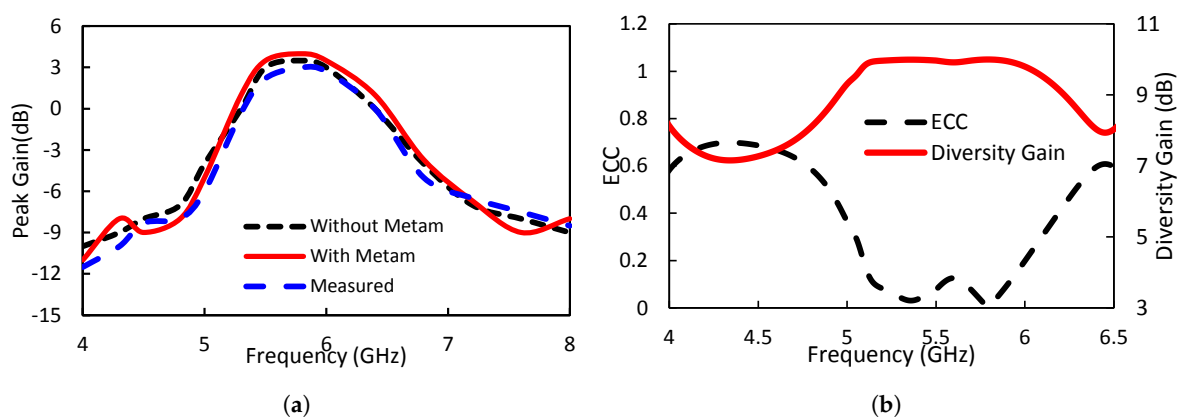


Figure 9. (a) Peak Gain of the proposed MIMO antenna, (b) ECC and Diversity Gain of the proposed antenna.

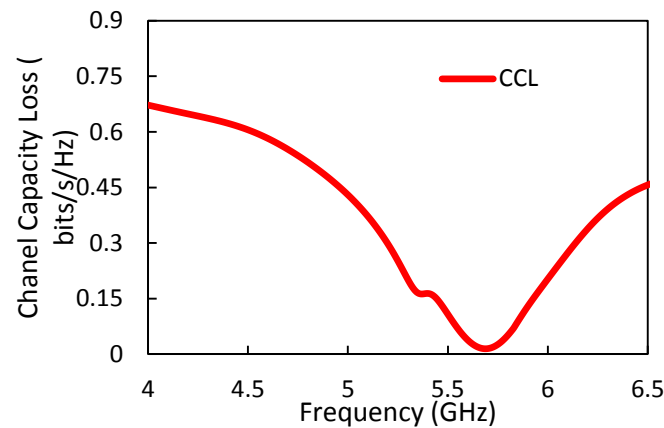


Figure 10. Channel Capacity Loss (CCL) of the proposed antenna.

#### 4. Conclusions

Throughout the scope of the presented paper, the design, prototyping, and measurement relating to a MIMO antenna, useful for MIMO applications, have been thoroughly depicted. The proposed antenna, operating at 5.8 GHz, has a simple structure with a size of  $44 \times 37 \text{ mm}^2$ . By incorporating metamaterial structure between the radiating patches of the MIMO antenna, a high isolation between the MIMO elements is achieved. The proposed antenna has good performances mainly in terms of Envelop Correlation Coefficient ( $ECC < 0.1$ ), Diversity gain ( $DG > 9 \text{ dB}$ ) and channel loss capacity ( $CCL < 0.05$ ) which make it as a potential candidate for MIMO system.

**Author Contributions:** A.I. and O.A.S. provided the idea, performed the experiments and managed the paper. A.B. (Amal Bouazizi) and A.B. (Abdul Basir) assisted in the idea development and paper writing.

**Funding:** This research received no external funding.

**Conflicts of Interest:** The authors declare no conflict of interest.

#### Abbreviations

The following abbreviations are used in this manuscript:

DG	Diversity Gain
MIMO	Multiple Input Multiple Output
dB	Decibel
ECC	Envelop Correlation Coefficient
CCL	Channel Capacity Loss

#### References

- Ludwig, A. Mutual coupling, gain and directivity of an array of two identical antennas. *IEEE Trans. Antennas Propag.* **1976**, *24*, 837–841. [[CrossRef](#)]
- Iqbal, A.; Saraereh, O.A.; Ahmad, A.W.; Bashir, S. Mutual Coupling Reduction Using F-Shaped Stubs in UWB-MIMO Antenna. *IEEE Access* **2018**, *6*, 2755–2759. [[CrossRef](#)]
- Su, S.W.; Lee, C.T.; Chang, F.S. Printed MIMO-antenna system using neutralization-line technique for wireless USB-dongle applications. *IEEE Trans. Antennas Propag.* **2012**, *60*, 456–463. [[CrossRef](#)]
- Ghosh, J.; Ghosal, S.; Mitra, D.; Bhadra Chaudhuri, S.R. Mutual coupling reduction between closely placed microstrip patch antenna using meander line resonator. *Prog. Electromagn. Res.* **2016**, *59*, 115–122. [[CrossRef](#)]
- Zhang, S.; Lau, B.K.; Sunesson, A.; He, S. Closely-packed UWB MIMO/diversity antenna with different patterns and polarizations for USB dongle applications. *IEEE Trans. Antennas Propag.* **2012**, *60*, 4372–4380. [[CrossRef](#)]
- Suntives, A.; Abhari, R. Miniaturization and isolation improvement of a multiple-patch antenna system using electromagnetic bandgap structures. *Microw. Opt. Technol. Lett.* **2013**, *55*, 1609–1612. [[CrossRef](#)]

7. Yu, A.; Zhang, X. A novel method to improve the performance of microstrip antenna arrays using a dumbbell EBG structure. *IEEE Antennas Wirel. Propag. Lett.* **2003**, *2*, 170–172.
8. Wu, W.; Yuan, B.; Wu, A. A Quad-Element UWB-MIMO Antenna with Band-Notch and Reduced Mutual Coupling Based on EBG Structures. *Int. J. Antennas Propag.* **2018**, *2018*, 8490740. [[CrossRef](#)]
9. Farsi, S.; Aliakbarian, H.; Schreurs, D.; Nauwelaers, B.; Vandenbosch, G.A. Mutual coupling reduction between planar antennas by using a simple microstrip U-section. *IEEE Antennas Wirel. Propag. Lett.* **2012**, *11*, 1501–1503. [[CrossRef](#)]
10. Zhu, F.G.; Xu, J.D.; Xu, Q. Reduction of mutual coupling between closely-packed antenna elements using defected ground structure. *Electron. Lett.* **2009**, *45*, 601–602. [[CrossRef](#)]
11. Chandel, R.; Gautam, A.K.; Rambabu, K. Design and Packaging of an Eye-Shaped Multiple-Input–Multiple-Output Antenna With High Isolation for Wireless UWB Applications. *IEEE Trans. Compon. Packag. Manuf. Technol.* **2018**, *8*, 635–642. [[CrossRef](#)]
12. Zhu, J.; Li, S.; Liao, S.; Xue, Q. Wideband Low-Profile Highly Isolated MIMO Antenna With Artificial Magnetic Conductor. *IEEE Antennas Wirel. Propag. Lett.* **2018**, *17*, 458–462. [[CrossRef](#)]
13. Liu, P.; Sun, D.; Wang, P.; Gao, P. Design of a Dual-Band MIMO Antenna with High Isolation for WLAN Applications. *Prog. Electromag. Res.* **2018**, *74*, 23–30. [[CrossRef](#)]
14. Sharawi, M.S. *Printed MIMO Antenna Engineering*; Artech House: Norwood, MA, USA, 2014.
15. Choukiker, Y.K.; Sharma, S.K.; Behera, S.K. Hybrid fractal shape planar monopole antenna covering multiband wireless communications with MIMO implementation for handheld mobile devices. *IEEE Trans. Antennas Propag.* **2014**, *62*, 1483–1488. [[CrossRef](#)]



© 2018 by the authors. Licensee MDPI, Basel, Switzerland. This article is an open access article distributed under the terms and conditions of the Creative Commons Attribution (CC BY) license (<http://creativecommons.org/licenses/by/4.0/>).